J|A|C|S
ARTICLES
Published on Web 09/29/2006

Lithium Diisopropylamide-Mediated Ortholithiation and Anionic Fries Rearrangement of Aryl Carbamates: Role of Aggregates and Mixed Aggregates

Kanwal Jit Singh and David B. Collum*

Contribution from the Department of Chemistry and Chemical Biology, Baker Laboratory, Cornell University, Ithaca, New York 14853-1301

Received June 30, 2006; E-mail: dbc6@cornell.edu

Abstract: Structural and mechanistic studies of the lithium diisopropylamide (LDA)-mediated anionic Fries rearrangements of aryl carbamates are described. Substituents at the meta position of the arene (H, OMe, F) and the dialkylamino moiety of the carbamate (Me_2N, Et_2N, and *i*-Pr_2N) markedly influence the relative rates of ortholithiation and subsequent Fries rearrangement. Structural studies using ^6Li and ^{15}N NMR spectroscopies on samples derived from [^6Li,^{15}N]LDA reveal an LDA dimer, LDA dimer−arene complexes, an aryllithium monomer, LDA−aryllithium mixed dimers, an LDA−lithium phenolate mixed dimer, and homoaggregated lithium phenolates. The highly insoluble phenolate was characterized as a dimer by X-ray crystallography. Rate studies show monomer- and dimer-based ortholithiations as well as monomer- and mixed dimer-based Fries rearrangements. Density functional theory computational studies probe experimentally elusive structural and mechanistic details.

Introduction

Fries rearrangements are approaching their centenary year.[1,2] The Lewis acid mediated version was discovered by Fries in 1908.[3] A photochemical variant was first described in 1960,[4] and the anionic variant appears to have been first reported by Melvin in 1981.[5] The synthetic utility of the anionic Fries rearrangement exemplified by the tandem ortholithiation−Fries rearrangement of aryl carbamate **1** (eq 1)[6] has come about from high yields and ortho specificity. The reaction has received attention from the pharmaceutical industry;[7] its increasingly widespread use derives in large part from extensive development by Snieckus and co-workers.[2]

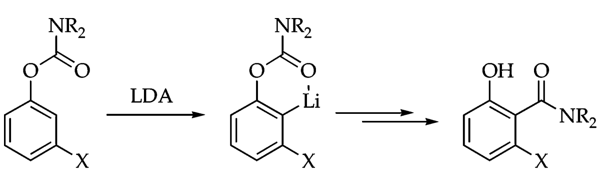

1 **2** **3** (1)

We describe herein structural and mechanistic investigations of the lithium diisopropylamide (LDA)-mediated Fries rearrangement illustrated in eq 1.[6] Spectroscopic studies reveal that the reaction proceeds through a number of intermediates summarized in Scheme 1. The choice of solvent and substrate dictates which intermediates can be observed as the reaction proceeds. Rate studies of both the ortholithiation and the subsequent rearrangement reveal some surprising consequences of mixed aggregation.

Results

The results are presented sequentially as follows: (1) relative reactivities—qualitative studies reveal how the meta substituent (X) and the carbamate substituent (NR_2) influence the relative rates of ortholithiations and Fries rearrangements; (2) aggregate structures—IR and NMR spectroscopic studies establish the structures of the intermediates in Scheme 1; (3) rate studies—concentration-dependent rates reveal the mechanism(s) of the LDA-mediated ortholithiations and the subsequent Fries rearrangements; and (4) computational studies—density functional theory (DFT) calculations provide insights into experimentally

(1) Blatt, A. H. *Chem. Rev.* **1940**, *27*, 413. Martin, R. *Org. Prep. Proc. Int.* **1992**, *24*, 369.
(2) (a) Hartung, C. G.; Snieckus, V. In *Modern Arene Chemistry*; Astruc, D., Ed.; Wiley-VCH: Weinheim, 2002; Chapter 10. (b) Snieckus, V. *Chem. Rev.* **1990**, *90*, 879. (c) Taylor, C. M.; Watson, A. J. *Curr. Org. Chem.* **2004**, *8*, 623.
(3) Fries, K.; Finck, G. *Ber.* **1908**, *41*, 2447.
(4) Anderson, J. C.; Reese, C. B. *Proc. Chem. Soc.* **1960**, 217.
(5) (a) Melvin, L. S. *Tetrahedron Lett.* **1981**, 3375. (b) For the first example of an aryl carbamate-derived anionic Fries rearrangement, see: Sibi, M. P.; Snieckus, V. *J. Org. Chem.* **1983**, *48*, 1935.
(6) Leading references: MacNeil, S. L.; Wilson, B. J.; Snieckus, V. *Org. Lett.* **2006**, *8*, 1133.
(7) (a) Nguyen, T.; Wicki, M. A.; Snieckus, V. *J. Org. Chem.* **2004**, *69*, 7816. (b) Mhaske, S. B.; Argade, N. P. *J. Org. Chem.* **2004**, *69*, 4563. (c) Harfenist, M.; Joseph, D. M.; Spence, S. C.; Mcgee, D. P. C.; Reeves, M. D.; White, H. L. *J. Med. Chem.* **1997**, *40*, 2466. (d) Piettre, A.; Chevenier, E.; Massardier, C.; Gimbert, Y.; Greene, A. E. *Org. Lett.* **2002**, *4*, 3139. (e) Dankwardt, J. W. *J. Org. Chem.* **1998**, *63*, 3753. (f) Mohri, S.; Stefinovic, M.; Snieckus, V. *J. Org. Chem.* **1997**, *62*, 7072. (g) Lampe, J. W.; Hughes, P. F.; Biggers, C. K.; Smith, S. H.; Hu, H. *J. Org. Chem.* **1994**, *59*, 5147. (h) Lampe, J. W.; Biggers, C. K.; Defauw, J. M.; Foglesong, R. J.; Hall, S. E.; Heerding, J. M.; Hollinshead, S. P.; Hu, H.; Hughes, P. F.; Jagdmann, G. E., Jr.; Johnson, M. G.; Lai, Y.-S.; Lowden, C. T.; Lynch, M. P.; Mendoza, J. S.; Murphy, M. M.; Wilson, J. W.; Ballas, L. M.; Carter, K.; Darges, J. W.; Davis, J. E.; Hubbard, F. R.; Stamper, M. L. *J. Med. Chem.* **2002**, *45*, 2624.

Scheme 1

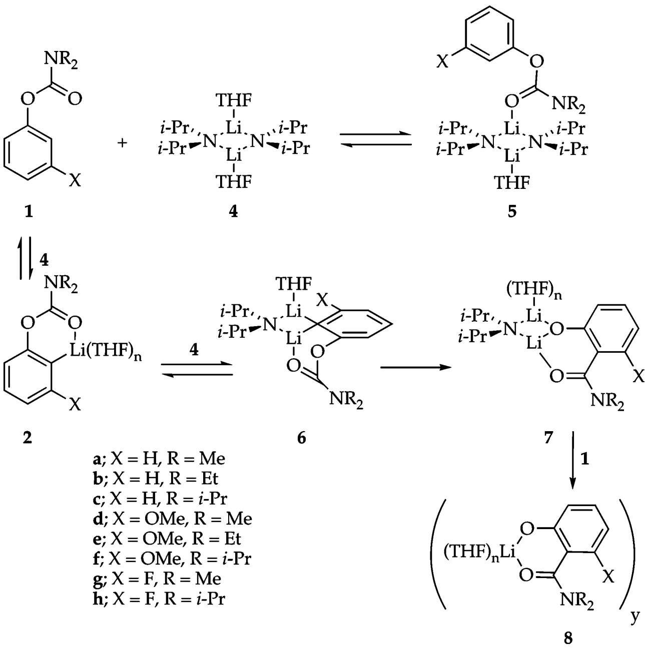

Table 1. ^{6}Li and ^{15}N NMR Spectral Data[a]

structure	^{6}Li, δ (mult, J_{LiN})	^{15}N, δ (mult)
7a	0.43 (d, 4.9)	78.1 (q)
6b	1.39 (d, 4.9)	
7b	0.44 (d, 4.9)	78.1 (q)
6c	1.51 (d, 5.1)	77.6 (q)
7c	0.50 (d, 5.0)	77.9 (q)
6d	1.68 (d, 5.1)	76.4 (q)
7d	0.41 (d, 5.0)	78.3 (q)
6e	1.70 (d, 5.1)	76.5 (q)
6f	1.69 (d, 5.0)	76.7 (q)
7f	0.62 (d, 5.0)	77.7 (q)
6g	1.71 (d, 5.3)	76.3 (q)
7g	0.40 (d, 4.8)	79.1 (q)
2g	1.22 (s)	
8g	0.73 (br)	
6h	1.79 (d, 5.3)	76.4 (q)
6d[b]	1.99 (d, 5.2)	75.3 (q)
7d[b]	0.90 (d, 5.6), 0.97 (d, 3.9)	
5d[c]	1.61 (t, 4.3), 1.85 (t, 5.3)	71.23 (q)

[a] Spectra were recorded on samples containing 0.10 M total lithium concentration (normality). Multiplicities are denoted as follows: s, singlet; d, doublet; t, triplet; q, quintet; m, multiplet; br, broad. The chemical shifts are reported relative to 0.3 M ^{6}LiCl/MeOH (0.0 ppm) and neat Me_2NEt (25.7 ppm) at −90 °C. All *J* values are reported in Hz. Unless otherwise indicated, solvent is 11.1 M THF/pentane. [b] Solvent is 2.3 M *n*-BuOMe. [c] Solvent is 6.3 M *t*-BuOMe.

elusive details. The transition structures depicted are also supported by previous computational studies of LDA-mediated lithiations.[8]

Relative Reactivities. Some qualitative observations pertaining to substituent effects provide a sense of how meta substituents on the arene and N-alkyl substituents on the carbamate moiety influence reactivity. The methods for measuring their relative reactivities are discussed below in the context of detailed rate studies.

Bulky carbamate substituents have limited influence on the rates of ortholithiation yet dramatically impact the rates of Fries rearrangement ($Me_2N \gg Et_2N \gg i\text{-}Pr_2N$).[2b] Consequently, arene **1a** bearing an Me_2N substituent and no anion stabilizing meta substituent affords a relatively slow (rate-limiting) ortholithiation followed by a rapid Fries rearrangement; the intermediate aryllithium (**2a** or **6a**) is not detected (see below). Conversely, ortholithiation of the corresponding *N*,*N*-diisopropyl carbamate **1c** occurs at −40 °C to the exclusion of the Fries rearrangement (eq 2) but proceeds to low (<10%) conversion as shown by in situ IR spectroscopy. Quantitative ortholithiation of **1c** using

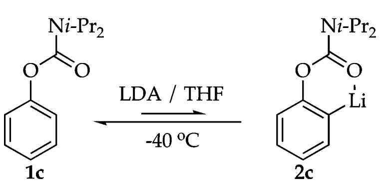

(2)

lithium tetramethylpiperidide at −40 °C and subsequent addition of *i*-Pr_2NH reverses the ortholithiation, confirming that the low conversion to aryllithium using LDA derives from an unfavorable equilibrium.

Electron-withdrawing substituents at the meta position markedly accelerate the ortholithiation. By example, carbamate **1g** ortholithiates with excess LDA instantly even at −78 °C. Conversely, Fries rearrangement starting from mixed dimer **6g** is 10-fold slower than from **6d**. Presumably both rate effects derive from inductive stabilization of the aryllithium.[9]

Aggregate Structures. LDA, [^{6}Li]LDA, and [^{6}Li,^{15}N]LDA were prepared as white crystalline solids.[10] Spectral data for the key structural forms depicted in Scheme 1 are summarized in Table 1. Representatives of the structural forms in Scheme 1 were documented through changes in substituents. ^{6}Li and ^{15}N assignments stem from ^{6}Li, ^{13}C, and ^{15}N NMR spectroscopies[11] augmented by ^1J(^{6}Li,^{15}N)-resolved[12] and ^{6}Li,^{15}N HMQC spectroscopies.[13] In situ IR spectra were recorded using a silicon-based probe.[14] LDA was previously shown to be disolvated dimer **4** at all THF concentrations.[11,15] By adjusting the substituents on both the arene and the carbamate, representatives of the different structural forms in Scheme 1 could be formed and characterized as follows.

We studied the complexation of carbamates to LDA using carbamate **1d** emblematically because of its role in the rate studies decribed below. IR spectra recorded on mixtures of 0.20 M LDA and 0.004 M carbamate **1d** in 0.70 M THF/hexane solution at −40 °C reveal the absorbance of uncoordinated **1d** at 1736 cm^{-1} along with an absorbance at 1714 cm^{-1}, consistent with LDA−carbamate complex **5d**. Uncoordinated carbamate **1d** is the sole observable form in ≥3.0 M THF. By contrast,

(8) (a) Romesberg, F. E.; Collum, D. B. *J. Am. Chem. Soc.* **1995**, *117*, 2166. (b) Ramirez, A.; Lobkovsky, E.; Collum, D. B. *J. Am. Chem. Soc*. **2003**, *125*, 15376. (c) Wiedemann, S. H.; Ramirez, A.; Collum, D. B. *J. Am. Chem. Soc.* **2003**, *125*, 15893.

(9) (a) Maggi, R.; Schlosser, M. *Tetrahedron Lett*. **1999**, *40*, 8797. (b) Schlosser, M.; Mongin, F.; Porwisiak, J.; Dmowski, W.; Büker, H. H.; Nibbering, N. M. M. *Chem.*−*Eur. J.* **1998**, *4*, 1281. (c) Schlosser, M. *Angew. Chem., Int. Ed.* **1998**, *37*, 1497. Büker, H. H.; Nibbering, N. M. M.; Espinosa, D.; Mongin, F.; Schlosser, M. *Tetrahedron Lett.* **1997**, *38*, 8519. (d) Chadwick, S. T.; Rennels, R. A.; Rutherford, J. L.; Collum, D. B. *J. Am. Chem. Soc.* **2000**, *122*, 8640.

(10) Kim, Y.-J.; Bernstein, M. P.; Galiano-Roth, A. S.; Romesberg, F. E.; Fuller, D. J.; Harrison, A. T.; Collum, D. B.; Williard, P. G. *J. Org. Chem.* **1991**, *56*, 4435.

(11) Collum, D. B. *Acc. Chem. Res.* **1993**, *26*, 227.

(12) Rutherford, J. L.; Collum, D. B. *J. Am. Chem. Soc.* **1999**, *121*, 10198.

(13) Xiang, B.; Winemiller, M. D.; Briggs, T. F.; Fuller, D. J.; Collum, D. B. *Magn. Reson. Chem.* **2001**, *39*, 137.

(14) Rein, A. J.; Donahue, S. M.; Pavlosky, M. A. *Curr. Opin. Drug Discovery Dev.* **2000**, *3*, 734.

(15) Remenar, J. F.; Lucht, B. L.; Collum, D. B. *J. Am. Chem. Soc.* **1997**, *119*, 5567 and references therein.

complexation of **1d** is quantitative using LDA in poorly coordinating[1] *t*-BuOMe (≤4.0 M) or *n*-BuOMe (<2.5 M). [^{6}Li]LDA and [^{6}Li,^{15}N]LDA of **5d** afford ^{6}Li and ^{15}N resonances and couplings consistent with the assigned structure (Table 1).

Arenes bearing electron-withdrawing MeO and F meta substituents undergo rapid and quantitative ortholithiation with excess LDA in THF at −78 °C to afford mixed dimers (**6**)[17] and low concentrations of aryllithiums (**2**). Lower THF concentrations promote mixed dimers to the exclusion of the aryllithium monomer. Mixed dimers display a highly characteristic ^{6}Li doublet and a ^{15}N quintet at −90 °C.[11,18] The ^{6}Li resonance of **6g** resolves into two resonances (1:1) at < −125 °C, consistent with chelation by the carbamate.

It proved difficult to characterize aryllithiums **2** because of low percent conversion in the ortholithiation, high reactivity toward Fries rearrangement in the absence of excess LDA, mixed dimer formation in the presence of excess LDA, and limited solubility in several instances. Only aryl carbamates **1g** and **1h**, bearing electron-withdrawing meta substituents, were quantitatively metalated with 1.0 equiv of LDA to give homoaggregated aryllithium (**2g** and **2h**, respectively). The absence of ^{15}N coupling in the ^{6}Li resonance confirms the absence of an LDA fragment. Unfortunately, limited solubility rendered ^{13}C NMR spectroscopy impractical; precedent suggests that such aryllithiums are monomeric.[19,20]

Fries rearrangement of mixed dimers (**6**) in the presence of excess LDA affords LDA−lithium phenolate mixed dimers (**7**). For example, mixed dimer **7a** prepared from [^{6}Li,^{15}N]LDA displays a single ^{6}Li resonance as a doublet.[11] Inequivalent ^{6}Li resonances arising from chelation in **7a** are not observed; however, site−site exchange is often fast on NMR time scales even at < −120 °C.

Homoaggregated phenolate **8** can be generated using equimolar mixtures of carbamate and LDA and by forcing the metalation to proceed beyond the formation of a mixed dimer. Unfortunately, a combination of profound insolubilities of **8** as a class and the absence of Li−X coupling precluded detailed characterization in solution. A crystal structure of **8g** (Figure 1) shows a dimer in analogy with other structurally similar phenolates.[21]

Rate Studies: Ortholithiation. The ortholithiation was studied according to eq 3. Pseudo-first-order conditions were established by maintaining the concentration of the carbamate **1a** at ≤0.004 M. LDA, and THF concentrations were maintained

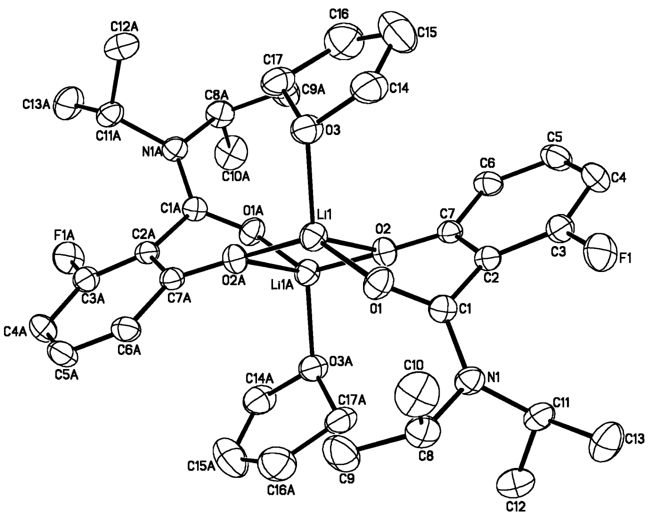

Figure 1. ORTEP of the lithium phenolate **8g**.

at high, yet adjustable, levels, using hexane as the cosolvent.[22] The loss of **1a** monitored using in situ IR spectroscopy follows

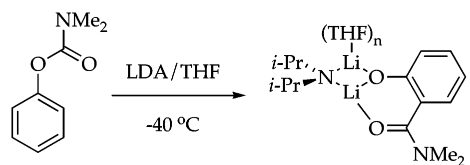

1a **7a** (3)

clean first-order behavior. The resulting pseudo-first-order rate constants (k_{obsd}) are independent of the initial concentration of **1a**, confirming a first-order dependence.[23] Under these conditions, there is no measurable buildup of an ortholithiated form, indicating a rate-limiting ortholithiation followed by a rapid Fries rearrangement. A significant isotope effect ($k_H/k_D = 16$) is found by comparing the independently measured rate constants for the elimination of **1a** and **1a-*d*$_5$**.[10d,24] Added diisopropylamine has no effect on the rates, confirming that the ortholithiations rather than the Fries rearrangements are rate limiting.

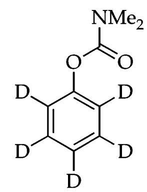

1a-*d*$_5$

Plots of k_{obsd} versus LDA concentration and k_{obsd} versus THF concentration (Figures 2 and 3) reveal half-order and zeroth-order dependencies, respectively. Overall, the reaction orders and the kinetic isotope effect are consistent with the idealized rate law in eq 4,

$$-d[\mathbf{1a}]/dt = k'[\mathbf{1a}][\mathrm{LDA}]^{1/2}[\mathrm{THF}]^0 \qquad (4)$$

the mechanism described generically in eqs 5 and 6,

(16) For other examples of spectroscopically observable LDA−substrate complexes, see: Sun, X.; Collum, D. B. *J. Am. Chem. Soc.* **2000**, *122*, 2452. Also, see ref 18b.
(17) Pratt, L. M. *Mini-Rev. Org. Chem.* **2004**, *1*, 209.
(18) (a) Sun, X.; Collum, D. B. *J. Am. Chem. Soc.* **2000**, *122*, 2459. (b) Ramirez, A.; Sun, X.; Collum, D. B. *J. Am. Chem. Soc.* **2006**, *128*, in press. (c) Romesberg, F. E.; Collum, D. B. *J. Am. Chem. Soc.* **1994**, *116*, 9198. (d) Galiano-Roth, A. S.; Kim, Y.-J.; Gilchrist, J. H.; Harrison, A. T.; Fuller, D. J.; Collum, D. B. *J. Am. Chem. Soc.* **1991**, *113*, 5053. (e) Sun, C.; Williard, P. G. *J. Am. Chem. Soc.* **2000**, *122*, 7829.
(19) (a) Ramirez, A.; Candler, J.; Bashore, C. G.; Wirtz, M. C.; Coe, J. W.; Collum, D. B. *J. Am. Chem.* Soc. **2004**, *126*, 14700. (b) Stratakis, M.; Wang, P. G.; Streitwieser, A. *J. Org. Chem.* **1996**, *61*, 3145. (c) Reich, H. J.; Green, D. P.; Medina, M. A.; Goldenberg, W. S.; Gudmundsson, B. O.; Dykstra, R. R.; Phillips, N. H. *J. Am. Chem. Soc.* **1998**, *120*, 7201.
(20) In contrast to some recently characterized ortho fluoro aryllithium monomers,[19a] the ^{6}Li resonance of **2g** shows no detectable ^{6}Li−^{19}F coupling.
(21) Wang, Z.; Chai, Z.; Li, Y. *J. Organomet. Chem.* **2005**, *690*, 4252. Boyle, T. J.; Pedrotty, D. M.; Alam, T. M.; Vick, S. C.; Rodriguez, M. A. *Inorg. Chem.* **2000**, *39*, 5133. Clegg, W.; Lamb, E.; Liddle, S. T.; Snaith, R.; Wheatley, A. E. H. *J. Organomet. Chem.* **1999**, *573*, 305. Cetinkaya, B.; Gumrukcu, I.; Lappert, M. F.; Atwood, J. L.; Shakir, R. *J. Am. Chem. Soc.* **1980**, *102*, 2086. Khanjin, N. A.; Menger, F. M. *J. Org. Chem.* **1997**, *62*, 8923.
(22) The concentration of the LDA, although expressed in units of molarity, refers to the concentration of the monomer unit (normality).
(23) Espenson, J. H. *Chemical Kinetics and Reaction Mechanisms*, 2nd ed.; McGraw-Hill: New York, 1995.
(24) Anderson, D. R.; Faibish, N. C.; Beak, P. *J. Am. Chem. Soc.* **1999**, *121*, 7553.

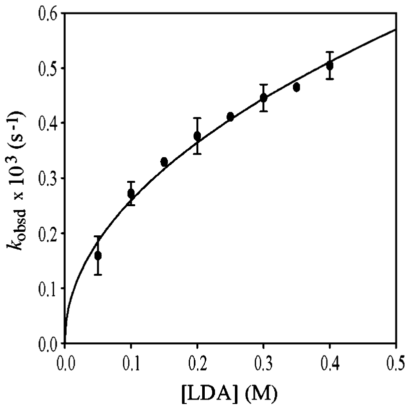

Figure 2. Plot of k_{obsd} versus [LDA] in 9.0 M THF/hexane for the ortholithiation of **1a-*d*$_5$** (0.0025 M) at −40 °C. The curve depicts an unweighted least-squares fit to $k_{obsd} = k[\mathrm{LDA}]^n$. $k = (8.0 \pm 0.4) \times 10^{-4}$, $n = 0.49 \pm 0.03$.

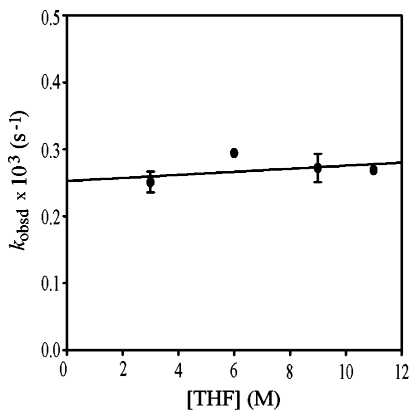

Figure 3. Plot of k_{obsd} versus [THF] in hexane cosolvent for the ortholithiation of **1a** (0.0025 M) by LDA (0.10 M) at −40 °C. The curve depicts an unweighted least-squares fit to $k_{obsd} = k[\mathrm{THF}] + k'$ [$k = (2.3 \pm 0.3) \times 10^{-6}$, $k' = (2.5 \pm 0.2) \times 10^{-4}$].

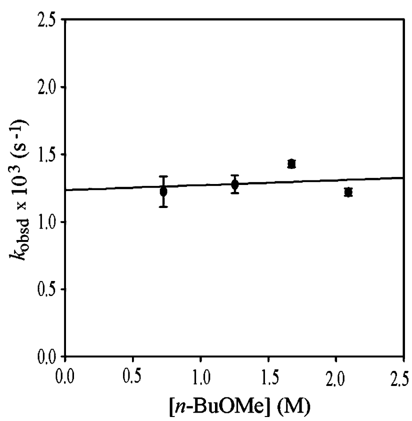

Figure 4. Plot of k_{obsd} versus [*n*-BuOMe] in hexane cosolvent for the ortholithiation of **5d** (0.004 M) by LDA (0.10 M) at −40 °C. The curve depicts an unweighted least-squares fit to $k_{obsd} = k[n\text{-BuOMe}] + k'$ [$k = (3.7 \pm 0.8) \times 10^{-5}$, $k' = (1.2 \pm 0.1) \times 10^{-3}$].

$$1/2\ (i\text{-Pr}_2\text{NLi})_2(\text{THF})_2 \rightleftharpoons (i\text{-Pr}_2\text{NLi})(\text{THF}) \qquad (5)$$

$$(i\text{-Pr}_2\text{NLi})(\text{THF}) + \mathbf{1a} \rightarrow [(i\text{-Pr}_2\text{NLi})(\text{THF})(\mathbf{1a})]^{\ddagger} \qquad (6)$$

and a monomer-based transition structure such as **9**.

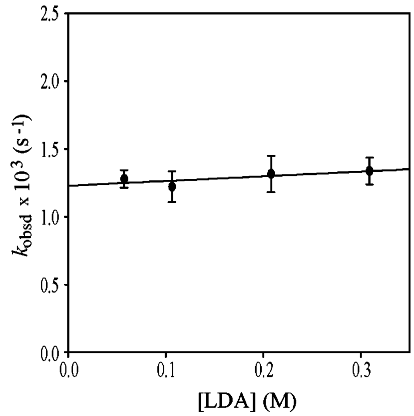

Figure 5. Plot of k_{obsd} versus [LDA] in 0.73 M *n*-BuOMe/hexane for the ortholithiation of **5d** (0.004 M) at −40 °C. The curve depicts an unweighted least-squares fit to $k_{obsd} = k[\mathrm{LDA}] + k'$ [$k = (3.5 \pm 0.3) \times 10^{-4}$, $k' = (1.20 \pm 0.07) \times 10^{-3}$].

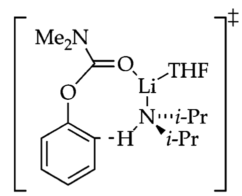

9

Analogous rate studies for the metalation of **1d** in ≤2.5 M *n*-BuOMe/hexane (eq 7) reveal a markedly different result. Under these conditions the observable starting material is monocomplexed dimer **5d**. Plots of k_{obsd} versus *n*-BuOMe

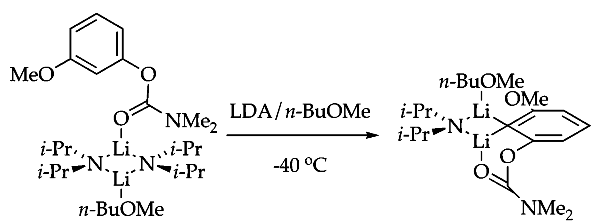

5d **6d** (7)

concentration (Figure 4) and k_{obsd} versus LDA concentration (Figure 5) afford the idealized rate law in eq 8, consistent with the mechanism depicted generically in eq 9

$$-\mathrm{d}[\mathbf{5d}]/\mathrm{d}t = k'[\mathbf{5d}][\mathrm{LDA}]^0[n\text{-BuOMe}]^0 \qquad (8)$$

$$\underset{(\mathbf{5d})}{(i\text{-Pr}_2\text{NLi})_2(n\text{-BuOMe})(\mathbf{1d})} \rightleftharpoons \underset{(\mathbf{10})}{[(i\text{-Pr}_2\text{NLi})_2(n\text{-BuOMe})(\mathbf{1d})]^{\ddagger}} \qquad (9)$$

and with open dimer-based transition structure **10**.[25] Of course, the marked changes in the concentration dependencies are, in part, a consequence of the starting form being an LDA−arene complex.[26] Nonetheless, the emergence of dimer-based reactivity

(25) For a bibliography of lithium amide open dimers, see ref 18b.

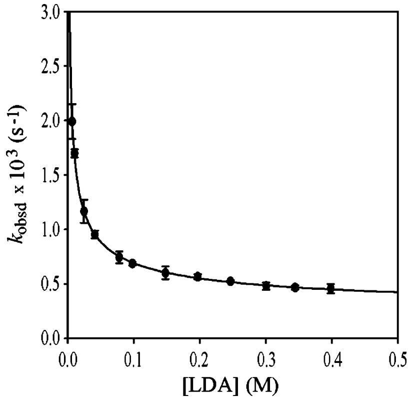

Figure 6. Plot of k_{obsd} versus [LDA] in 9.8 M THF/hexane for the Fries rearrangement of **1g** (0.004 M) at −40 °C. The curve depicts an unweighted least-squares fit to $k_{obsd} = k\,[\mathrm{LDA}]^n + k'$ [$k = (1.7 \pm 0.3) \times 10^{-4}$, $k' = (1.9 \pm 0.7) \times 10^{-4}$, $n = -0.48 \pm 0.04$].

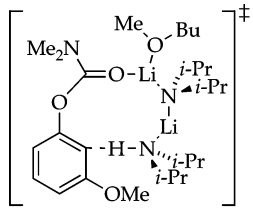

10

represents a fundamental change in mechanism affiliated with a change to a poorly coordinating solvent.[27]

Rate Studies: Fries Rearrangement. Fluorinated carbamate **1g** offered the best view of the anionic Fries rearrangement (eq 10).[28] We generated mixed aggregate **6g** as a 0.004 M solution in THF at −40 °C by adding **1g** to an excess of LDA. (The fluoro substituent ensured quantitative metalation at −78 °C.) The loss of **6g** and the formation of **7g** follow clean first-order behavior. The resulting values of k_{obsd} are independent of the

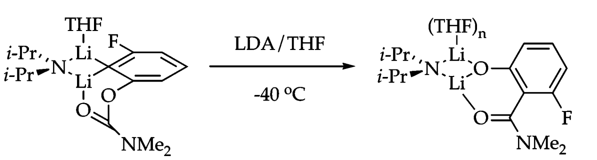

6g **7g** (10)

initial concentration of **6g**, confirming the first-order dependence. The decays also follow first-order dependencies, as shown by their least-squares fits to the nonlinear Noyes equation.[29] A plot of k_{obsd} versus LDA concentration (Figure 6) reveals two mechanisms: (1) an *inverse* half-order dependence on LDA concentration consistent with a mechanism requiring mixed aggregate dissociation[30] and (2) a zeroth-order dependence consistent with a mixed dimer-based rearrangement.[23] Plots of k_{obsd} versus THF concentration (Figures 7 and 8) reveal a first-order dependence at high LDA concentration (affiliated with the nondissociative mechanism) and a second-order dependence at low LDA concentration (affiliated with the dissociative mechanism).[31] The reaction orders are consistent with the idealized rate law in eq 11, the mechanisms described generically in eqs 12−14,

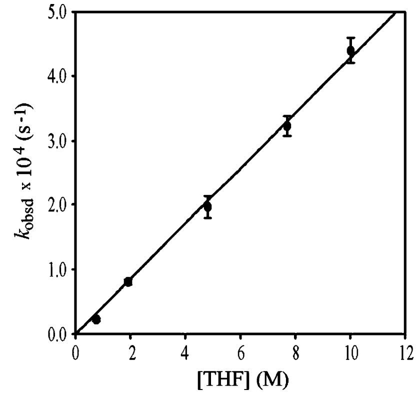

Figure 7. Plot of k_{obsd} versus [THF] in hexane cosolvent for the Fries rearrangement of **1g** (0.004 M) by LDA (0.42 M) at −40 °C. The curve depicts an unweighted least-squares fit to $k_{obsd} = k[\mathrm{THF}]^n$ [$k = (3.6 \pm 0.4) \times 10^{-5}$, $n = 1.08 \pm 0.05$].

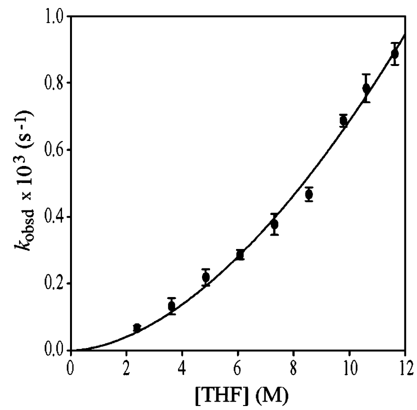

Figure 8. Plot of k_{obsd} versus [THF] in hexane cosolvent for the Fries rearrangement of **1g** (0.004 M) by LDA (0.098 M) at −40 °C. The curve depicts an unweighted least-squares fit to $k_{obsd} = k[\mathrm{THF}]^n$ [$k = (1.2 \pm 0.2) \times 10^{-5}$, $n = 1.75 \pm 0.07$].

$$-d[\mathbf{6g}]/dt = k'[\mathbf{6g}][\mathrm{THF}]^2[\mathrm{LDA}]^{-1/2} + k''[\mathbf{6g}][\mathrm{THF}][\mathrm{LDA}]^0 \qquad (11)$$

$$\underset{\mathbf{6g}}{(i\text{-}Pr_2NLi)(ArLi)(THF)} + 2THF \rightleftharpoons (ArLi)(THF)_2 + {}^1/_2(i\text{-}Pr_2NLi)_2(THF)_2 \qquad (12)$$

$$(ArLi)(THF)_2 \rightarrow \underset{\mathbf{11}}{[(ArLi)(THF)_2]^\ddagger} \qquad (13)$$

(26) Edwards, J. O.; Greene, E. F.; Ross, J. *J. Chem. Educ.* **1968**, *45*, 381.
(27) Zhao, P.; Collum, D. B. *J. Am. Chem. Soc.* **2003**, *125*, 4008. Zhao, P.; Collum, D. B. *J. Am. Chem.* Soc. **2003**, *125*, 14411.
(28) Carbamate **1d** forms a complex with LDA (**5d**). Subsequent ortholithiation of **5d** with LDA in *t*-BuOMe at −55 °C is first order in LDA with a significant nonzero intercept. The nonzero intercept is consistent with a pathway which is zero order in LDA as described for the ortholithiation of **5d** by LDA/*n*-BuOMe. LDA dependence, however, implicates a role of LDA that is quite unusual and as discussed in a forthcoming manuscript.
(29) Briggs, T. F.; Winemiller, M. D.; Collum, D. B.; Parsons, R. L., Jr.; Davulcu, A. K.; Harris, G. D.; Fortunak, J. D.; Confalone, P. N. *J. Am. Chem. Soc.* **2004**, *126*, 5427.
(30) Related inverse half-order dependencies on LDA concentration were observed in the context of ester enolization by LDA−lithium enolate mixed dimers.[18b]
(31) Fitting the data to $y = a[\mathrm{THF}]^n$ affords $a = (1.2 \pm 0.2) \times 10^{-5}$, $n = 1.75 + 0.07$. Alternatively, fits to $y = a[\mathrm{THF}]^n + c$ to account for a small but possible nonzero intercept affords $a = (7.0 \pm 3.0) \times 10^{-6}$, $n = 1.96 \pm 0.17$, and $c = (4.1 \pm 2.7) \times 10^{-5}$. A last perspective is provided by a fit to $y = a[\mathrm{THF}] + b[\mathrm{THF}]^n$, affording $a = (2.7 \pm 1.0) \times 10^{-5}$, $b = (1.4 \pm 1.9) \times 10^{-6}$, $n = 2.5 \pm 0.5$.

$$(i\text{-}Pr_2NLi)(ArLi)(THF) + THF \rightarrow [(i\text{-}Pr_2NLi)(ArLi)(THF)_2]^{\ddagger} \quad (14)$$

6g → **12**

and transition structures **11** and **12**. The solvation number assigned to **6g** is based on DFT calculations (below). Thus, the solvation number of **11** and **12** should be viewed as tentative.

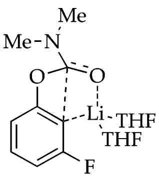

11

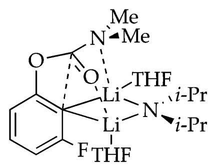

12

Computational Studies: General. We addressed several lingering issues using density functional theory calculations [B3LYP method and the 6-31G(d) basis set].[32] Corrections for entropy afforded the energy denoted as $\Delta G^{\ddagger}$ (activation energy). Me_2NLi and Me_2O were used as models for LDA and THF, respectively. Ranges of initial geometries were sampled for all reactant and transition structures. Legitimate saddle points were shown by the existence of single imaginary frequencies. Intrinsic reaction coordinate analyses verified that transition structures corresponded to desired transformations. To make comparisons with experiment as direct as possible, we focused on carbamate **1a** for the monomer-based ortholithiations, carbamate **1d** for the dimer-based ortholithiations, and carbamate **1g** for the Fries rearrangement.

Computational Studies: Ortholithiation. Disolvated dimer **13** is the reference state for the values of $\Delta G^{\ddagger}$ for the monomer-based ortholithiation (eq 15). The monosolvated monomer-based

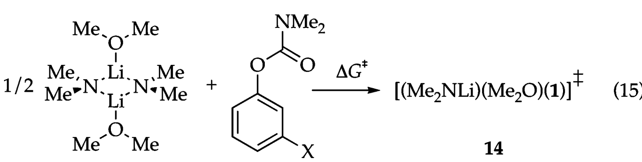

13 **1a**; X = H **1g**; X = F **14**

transition structure **14a** for the metalation of carbamate **1a** was implicated by the rate studies. Computations show a strong penchant for coordination by the carbonyl group; a variety of uncomplexed carbonyl orientations converge on **14a**. The N−H−C angle of **14a** is nearly 180°, consistent with a preference for linear proton transfer.[33]

The influence of electron-withdrawing groups probed using fluorinated carbamate **1g** revealed transition structure **14g** with a 5 kcal/mol reduction in $\Delta G^{\ddagger}$ when compared with the unsubstituted case. The influence of fluorine in facilitating the metalation via **14g** is probably inductive. By comparison, the ortholithiation via fluoro-directed analogue **15** is only slightly less favorable than that via **14g**. Similar effects have been noted previously.[9] Conversely, comparing the $\Delta G^{\ddagger}$ for **15** with the analogous $\Delta G^{\ddagger}$ for the directed metalation of fluorobenzene

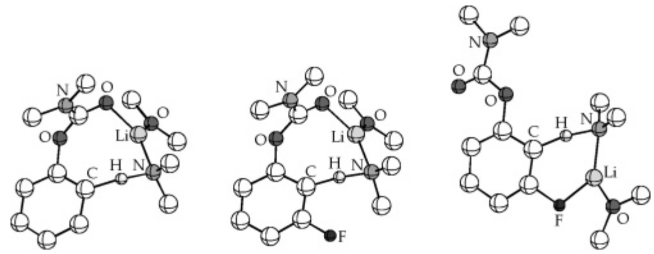

14a $\Delta G^{\ddagger}$ = 26.9 kcal/mol **14g** $\Delta G^{\ddagger}$ = 21.9 kcal/mol **15** $\Delta G^{\ddagger}$ = 22.8 kcal/mol

shows that the noncoordinating carbamate group facilitates the ortholithiation by approximately 3 kcal/mol.

We briefly examined the dimer-based metalations shown to occur from an observable complex in weakly coordinating solvents (eq 16).

$$\mathbf{1} + (Me_2NLi)_2(Me_2O)_2 \xrightarrow{\Delta G^{\ddagger}} [(Me_2NLi)_2(Me_2O)(\mathbf{1})]^{\ddagger} + Me_2O \quad (16)$$

13 → **16**

Although we use uncomplexed dimer **13** as the reference state (rather than a lithium amide dimer−arene complex as observed experimentally), substitution of **1** for an Me_2O ligand on dimer **13** is endothermic by <1.0 kcal/mol. Transition structures for dimer-based ortholithiations of the unsubstituted and methoxy-substituted carbamates are illustrated as **17** and **18**. The open-

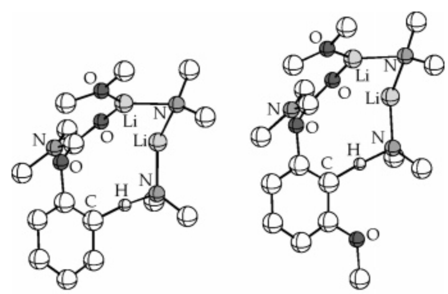

17 $\Delta G^{\ddagger}$ = 26.5 kcal/mol **18** $\Delta G^{\ddagger}$ = 26.4 kcal/mol

dimer motif has been implicated computationally on many occasions.[8,25] The most intriguing observation is that the methoxy moiety offers little stabilization when compared with the unsubstituted carbamate. According to the calculations, a methoxy moiety does not facilitate the carbamate metalation. This lack of activation by an ancillary (noncoordinating) meta methoxy moiety has been noted previously.[9d]

Computational Studies: Fries Rearrangement. Fries rearrangement starting with mixed dimer **6g** appeared to proceed via both a dissociative (monomer-based) pathway and a non-dissociative (mixed dimer-based) pathway (**11** and **12**, respectively). Modeling the reaction using mixed dimer **19** reveals that the most favorable monomer-based pathway (via disolvate **20**; eq 17) and the most favorable mixed dimer-based pathway (via disolvate **21**; eq 18)

(32) Frisch, M. J., et al. *Gaussian 03*, revision B.04; Gaussian, Inc.: Wallingford, CT, 2004.
(33) Bell, R. P. *The Tunnel Effect in Chemistry*; Chapman and Hall: New York, 1980.

$$\mathbf{19} + 2\mathrm{Me_2O} \xrightarrow{\Delta G^{\ddagger}} [(\mathrm{ArLi})(\mathrm{Me_2O})_2]^{\ddagger} + {}^{1}/_{2}\,\mathbf{13} \quad (17)$$
$$(\mathbf{20})$$

$$\mathbf{19} + \mathrm{Me_2O} \xrightarrow{\Delta G^{\ddagger}} [(\mathrm{ArLi})(\mathrm{Me_2NLi})(\mathrm{Me_2O})_2]^{\ddagger} \quad (18)$$
$$(\mathbf{21})$$

have comparable activation energies. Interestingly, **21** shows evidence of both N−Li *and* O−Li (η^2) coordination to lithium.[34]

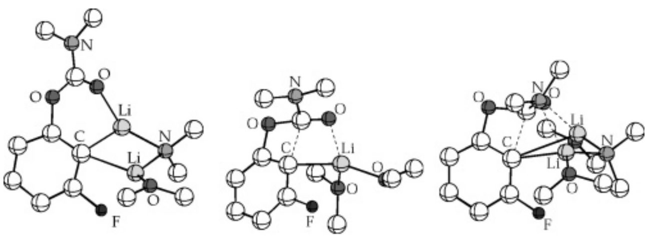

19 **20** $\Delta G^{\ddagger}$ = 32.9 kcal/mol **21** $\Delta G^{\ddagger}$ = 32.5 kcal/mol

Discussion

Summary. The tandem ortholithiation−Fries rearrangement depicted generically in eq 1 was studied at several levels. Qualitative IR spectroscopic studies revealed that the meta substituents on the arene ring and the alkyl groups on the carbamoyl moiety influence metalation and rearrangement rates. Electron-withdrawing meta substituents accelerate the lithiation, allow it to proceed to full conversion, and retard the subsequent Fries rearrangement—all consistent with a stabilized aryllithium. The alkyl substituents on the carbamate group have little influence on the ortholithiation but show marked effects on the Fries rearrangement; large alkyl groups retard the rearrangement.

NMR spectroscopic studies revealed an assortment of species summarized in Scheme 1. Judicious choices of substrate and reaction conditions were required to document the different structural forms. Poorly coordinating solvents, for example, promote LDA−arene complex **5**. Aryl carbamates bearing electron-withdrawing meta substituents (MeO or F) and only 1.0 equiv of LDA are required to form aryllithium **2** as the predominant species. Metalation of aryl carbamates with excess LDA affords mixed dimer **6** as the major species. Fries rearrangement in the presence of excess LDA affords **7**, whereas the analogous rearrangement in the absence of excess LDA affords **8**. Although dimer **4** and mixed aggregates **5**−**7** are rigorously characterized, limited solubility rendered the assignment of **2** incomplete and dependent on analogy with other aryllithiums. Profoundly low solubility of **8** and the absence of Li−X coupling rendered NMR spectroscopy useless; X-ray crystallography showed a dimer (Figure 1), as noted for related derivatives.[21]

Detailed rate studies of the ortholithiation of **1a** reveal that the metalation proceeds via monosolvated monomer-based transition structure **9**. Metalation in a poorly coordinating solvent (*n*-BuOMe) starting from an LDA dimer−arene complex analogous to **5** proceeds via monosolvated dimer-based transition structure **10**. The Fries rearrangement of mixed dimer **6**, a rare example of a carefully delineated mixed aggregate-based reaction, proceeds via both dissociative and nondissociative pathways via transition structures **11** and **12** (respectively).

Computational studies using Me_2NLi and Me_2O as models for LDA and THF, respectively, provide support to the proposed transition structures described above; these studies also offer experimentally elusive structural and energetic details. The most stable monomer-based transition structure for the metalation of carbamate **1a** is monosolvate **14a** consistent with experiment. Acceleration by fluorine is confirmed and is consistent with strong inductive effects. Moreover, the versatility of fluoro groups as ortho directors is supported by computations showing that a fluorine-directed ortholithiation is competitive (cf., **14g** and **15**). By contrast, an ancillary methoxy moiety offers little or no cooperative assistance to a carbamate-directed ortholithiation. The computational studies also provided insights into the Fries rearrangements. Both aryllithium monomer- and mixed-dimer-based rearrangements appear viable, as found experimentally.

On the Role of Mixed Aggregates. Mixed aggregation introduces a complexity whose prevalence and importance is easily underestimated.[35] Odd solvent effects or demands for excess organolithium reagents are easily dismissed as mysteries of science, but they have firm structural and mechanistic origins that can be elucidated with some effort. We have noticed, for example, that Snieckus and co-workers, the most avid users of Fries rearrangements, use excess LDA with great success.[2,7] Underneath this success lie interesting phenomena. Using only 1.0 equiv of LDA causes the metalation to stall owing to the buildup of mixed aggregates and affiliated autoinhibition.[18a,b] Conversely, the Fries rearrangement is faster in the absence of LDA. Thus, in this two-step sequence, excess LDA promotes the first step and retards the second. Although this conflict is not fatal—the reaction works quite well overall—it illustrates the complexities of such two-step protocols.

On the Role of "Precomplexes". The notion that Lewis basic functionalities on a substrate can interact with a metal in the rate limiting transition structures to facilitate organometallic reactions, the complex-induced proximity effect (CIPE), is widely accepted.[36] Mechanistic discussions of a heteroatom-directed ortholithiation, for example, are dominated by concerns about the role of substituent-lithium interactions in fostering ortholithiation.[2,36] Indeed, the computational support for a distinct carbonyl−lithium interaction in the rate-limiting transition structures such as **9** and **10** is convincing. There is, however, a tendency to ascribe importance to *transiently formed* complexes *preceding* the rate-limiting step. Such "precomplexes" are often construed as critical to preorganizing the species undergoing reaction. *To invoke such an interpretation of the CIPE is to ascribe a path* dependence that is invalid.[37] Any

(34) For additional discussion of the Lewis basicity of carboxamides on nitogen, see: Cox, C.; Young, V. G., Jr.; Lectka, T. *J. Am. Chem. Soc.* **1997**, *119*, 2307. Cox, C.; Ferraris, D.; Murthy, N. N.; Lectka, T. *J. Am. Chem. Soc.* **1996**, *118*, 5332.

(35) For leading references and discussions of mixed aggregation effects, see: (a) Seebach, D. *Angew. Chem., Int. Ed. Engl.* **1988**, *27*, 1624. (b) Tchoubar, B.; Loupy, A. *Salt Effects in Organic and Organometallic Chemistry*; VCH: New York, 1992; Chapters 4, 5, and 7. (c) Briggs, T. F.; Winemiller, M. D.; Xiang, B.; Collum, D. B. *J. Org. Chem.* **2001**, *66*, 6291. (d) Caubere, P. *Chem. Rev.* **1993**, *93*, 2317.

(36) For detailed discussions of complex-induced proximity effects, chelation effects, and other synonymous influences of internal ligation, see: (a) Whisler, M. C.; MacNeil, S.; Snieckus, V.; Beak, P. *Angew. Chem., Int. Ed.* **2004**, *43*, 2206. (b) Beak, P.; Meyers, A. I. *Acc. Chem. Res.* **1986**, *19*, 356. (c) Hay, D. R.; Song, Z.; Smith, S. G.; Beak, P. *J. Am. Chem. Soc.* **1988**, *110*, 8145. (d) Gronert, S.; Streitwieser, A., Jr. *J. Am. Chem. Soc.* **1988**, *110*, 2843. (e) Chen, X.; Hortelano, E. R.; Eliel, E. L.; Frye, S. V. *J. Am. Chem. Soc.* **1992**, *114*, 1778. (f) Das, G.; Thornton, E. R. *J. Am. Chem. Soc.* **1990**, *112*, 5360. (g) Klumpp, G. W. *Recl. Trav. Chim. Pays-Bas* **1986**, *105*, 1.

(37) Concerns over the interpretation of the CIPE have been noted previously. van Eikema Hommes, N. J. R.; Schleyer, P. v. R. *Angew. Chem., Int. Ed. Engl.* **1992**, *31*, 755. Collum, D. B. *Acc. Chem. Res.* **1992**, *25*, 448.

number of transiently formed species can *precede* the rate limiting step; none is kinetically relevant.

What are the consequences of observable LDA−arene complex **5**? Was it not the formation of **5** and an affiliated preorganization that diverted the metalation from a monomer- to a dimer-based pathway? In a word, no. The relative efficacies of the monomer- and dimer-based metalations are described by eq 19. The solvent-dependent change in mechanism—the

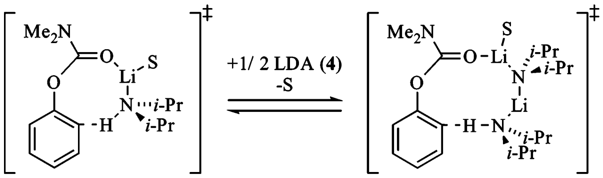

9 **10** (19)

solvent-dependent relative preferences for **9** versus **10**—derives from the energetic cost of solvent dissociation, a cost that is relatively low for weakly coordinating solvents. Observable complexation to form **5** also depends on the cost of solvent dissociation. Thus, observable complexation and a preference for dimer-based metalation share a common "lurking" variable,[38] solvent dissociation, but there is no direct causal relationship between complexation and dimer-based reaction.[37]

Conclusions

As mechanistic organic chemists, we are enamored with the elegance of the structural and mechanistic complexity accompanying the tandem ortholithiation−Fries rearrangement. The dual role of LDA−ArLi mixed aggregates as inhibitors of both the ortholithiation and the Fries rearrangement offers an unusually clear and rare view into mixed aggregation effects. We are reminded that simplistic mechanistic models to explain product distributions are quite likely to be wrong. The picture of relentless complexity, however, may frustrate those looking for prompt, simple answers. In our opinion, the principles emerging from detailed organolithium mechanistic studies are very rational, even enlightening, but neither punctuality nor simplicity is guaranteed.

So are these results merely curiosities? Synthetic chemists have done a remarkable job empirically tuning complex organolithium reactions to render them widely useful. The anionic Fries rearrangement has been *very* dependable without accompanying structural mechanistic insights. That is not to say, however, that empirical methods are necessarily optimized. Reactions that may have stalled inexplicably, for example, appear to have been achieved by simply adding excess base or warming the reaction vessel. Suppose, however, that using excess LDA is not an option. Poorly coordinating solvents may help; whereas ortholithiations of substrate **1c** in LDA/THF proceed to <10% conversion at equilibrium, LDA/Me_2NEt proceeds to >90% conversion. What if the Fries reaction is an unwanted side reaction of an ortholithiation−functionalization sequence? Can one promote the ortholithiation while precluding the Fries rearrangement? Hindered carbamates will do this, of course, but changing the substrate is not always an option. The zeroth-order THF dependence on the ortholithiation in conjunction with the second-order THF dependence on the Fries shows how lower solvent concentrations or poorly coordinating solvents selectively inhibit the Fries. Ortholithiation is also promoted relative to the Fries by excess LDA. Order of addition may be critical. What if benzyne formation becomes competitive on the halogenated substrates? Previous studies of ortholithiated dihalobenzenes show that benzyne formation is zeroth order in THF for LiCl elimination and inverse-first order in THF for elimination of LiF.[19a] The second-order dependence of the Fries rearrangement on the THF concentration suggests that strongly coordinating solvents should promote the Fries rearrangement. The extent to which the ortholithiation and the subsequent Fries rearrangement are fundamentally different processes suggests one should view them as such.

Experimental Section

Reagents and Solvents. THF, hexane, and pentane were distilled from blue or purple solutions containing sodium benzophenone ketyl. The hydrocarbon stills contained 1% tetraglyme to dissolve the ketyl. Crystalline LDA[10] was prepared from *n*-BuLi.[39] Air- and moisture-sensitive materials were manipulated under argon or nitrogen using standard glovebox, vacuum line, and syringe techniques. Solutions of *n*-BuLi and LDA were titrated using a literature method.[40] Substrates were prepared by literature procedures.[41]

NMR Spectroscopic Analyses. All NMR tubes were prepared using stock solutions and sealed under a partial vacuum. Standard ^{6}Li, ^{13}C, and ^{15}N NMR spectra were recorded on a 500 MHz spectrometer at 76.73, 125.79, and 50.66 MHz (respectively). The ^{6}Li, ^{13}C, and ^{15}N resonances are referenced to 0.3 M [^{6}Li]LiCl/MeOH at −90 °C (0.0 ppm), the CH_2O resonance of THF at −90 °C (67.57 ppm), and neat Me_2NEt at −90 °C (25.7 ppm), respectively.

IR Spectroscopic Analyses. Spectra were recorded using an in situ IR spectrometer fitted with a 30-bounce, silicon-tipped probe. The spectra were acquired in 16 scans at a gain of 1 and a resolution of 8 cm^{-1}. A representative reaction was carried out as follows: The IR probe was inserted through a nylon adapter and O-ring seal into an oven-dried, cylindrical flask fitted with a magnetic stir bar and a T-joint. The T-joint was capped by a septum for injections and an argon line. Following evacuation under a full vacuum and flushing with argon, the flask was charged with a solution of LDA (108.2 mg, 1.01 mmol) in THF/hexane (10.0 mL) and cooled in a temperature-controlled bath. After recording a background spectrum, a carbamate (**1**) was added to the LDA/THF mixture at −78 °C from a dilute stock solution (100 μL, 0.404 M) with stirring. IR spectra were recorded over the course of the reaction. To account for mixing and temperature equilibration, spectra recorded in the first 1.5 min were discarded. All reactions were monitored to >5 half-lives.

Acknowledgment. We thank the National Institutes of Health and the National Science Foundation for direct support of this work. We also thank Merck, Pfizer, Boehringer-Ingelheim, R. W. Johnson, Sanofi-Aventis, Schering-Plough, and DuPont Pharmaceuticals (Bristol-Myers Squibb) for indirect support. We also thank Emil Lobkovsky for determining two crystal structures.

Supporting Information Available: NMR spectra, rate and computational data, experimental protocols, and complete ref 32. This material is available free of charge via the Internet at http://pubs.acs.org.

JA064655X

(38) "Common response" or "lurking variable": Ryan, T. P. *Modern Regression Methods*; John Wiley: New York, 1996. Huff, D. *How to Lie with Statistics*; W. W. Norton: New York, 1993.
(39) *n*-Butyllithium can be recrystallized: (a) Hoffmann, D.; Collum, D. B. *J. Am. Chem. Soc.* **1998**, *120*, 5810. (b) Kottke, T.; Stalke, D. *Angew. Chem., Int. Ed. Engl.* **1993**, *32*, 580.
(40) Kofron, W. G.; Baclawski, L. M. *J. Org. Chem.* **1976**, *41*, 1879.
(41) Lustig, E.; Benson, W. R.; Duy, N. *J. Org. Chem.* **1967**, *32*, 851. Yamagami, C.; Takao, N.; Nishioka, T.; Fujita, T.; Takeuchi, Y. *Org. Magn. Reson.* **1984**, *22*, 439.